have reported findings that support the idea that reticular pseudodrusen may represent choroidal changes. Sohrab and associates[18] reported that correlation of registered IR, FAF, and red-free images localized the reticular pattern to the intravascular choroidal stroma on en face OCT sections. Querques and associates[17] showed that the reticular patterns appeared as hypofluorescent lesions on IA, closely abutting but not overlying the large choroidal vessels. Thus, although further investigations are necessary to determine the exact origin of reticular pseudodrusen, choroidal involvement should be taken into consideration to its pathogenesis.

Several studies have reported the abnormalities in the choroidal vascular structure in eyes with reticular pseudodrusen. A histologic report showed that small choroidal blood vessels were almost absent and larger vessels were also decreased in an eye with reticular pseudodrusen.[2] Another histologic report showed patchy loss of choroidal capillaries and a thin choroid in a pathologic specimen of reticular pseudodrusen.[4] In the current study, en face high-penetration SS-OCT images revealed that the choroidal vascular area of the Haller layer was decreased in eyes with reticular pseudodrusen but without CNV or geographic atrophy, compared with normal eyes. Taken together, our in vivo findings and previous histopathology data suggest that there may be a diffuse loss of small and large choroidal vessels, including choroidal capillaries, in eyes with reticular pseudodrusen, leading to choroidal thinning and reduced volume in the whole macular area prior to the development of CNV or geographic atrophy. Although choroidal thinning or reduced choroidal volume does not necessarily imply choroidal ischemia, these results suggest that atrophy of the whole choroid may be involved in the occurrence or development of reticular pseudodrusen. The reduction of ischemic factors, such as reducing cholesterol/triglyceride levels, controlling blood pressure, and taking anticoagulant agents, may be a therapeutic strategy for slowing choroidal atrophy and ultimately reducing the risk for late AMD in patients with reticular pseudodrusen. Further studies are necessary to evaluate the relationship between the progression to late AMD, systemic diseases, and reticular pseudodrusen.

There are several limitations of this study. Although high-penetration SS-OCT increases the sensitivity of the choroid, light is still scattered by the RPE and choroid, which makes visualization of the choriosclera interface difficult in a few images. In the current study, in B-scans where it was difficult to identify the whole outer choroid, 7-15 points where the choriosclera interface could be identified were chosen and connected to create a segmentation line. There was no automated segmentation software available for measuring choroidal thickness for the SS-OCT prototype system; thus, all segmentations were performed manually. However, we have previously shown good interobserver repeatability with this technique.[28] Because this was a cross-sectional study, we might have overlooked stage 4 reticular pseudodrusen (fading of the subretinal material because of reabsorption and migration within the inner retinal layers).[40] Recently, using multimodal imaging, Spaide[41] demonstrated that eyes with regression of reticular pseudodrusen develop outer retinal atrophy and loss of the underlying choroidal thickness. Thus, further assessment is necessary to evaluate the choroidal changes in stage 4 of reticular pseudodrusen.

In conclusion, our study revealed that macular choroidal thickness and volume in eyes with reticular pseudodrusen were significantly decreased, regardless of CNV or geographic atrophy. Furthermore, en face SS-OCT images showed that the choroidal vascular area was decreased in eyes with reticular pseudodrusen. Although it remains unknown whether choroidal thinning and choroidal vascular changes are causes or consequences of reticular pseudodrusen, the findings of this study may help to elucidate its pathogenesis. In the future, we hope to perform longitudinal studies using SS-OCT to further elucidate the involvement of the choroid in the pathogenesis of reticular pseudodrusen.

ALL AUTHORS HAVE COMPLETED AND SUBMITTED THE ICMJE FORM FOR DISCLOSURE OF POTENTIAL CONFLICTS OF INTEREST. Financial disclosures: Nagahisa Yoshimura: advisory board of Topcon. This research was supported in part by the Grant-in-Aid for Scientific Research (21791679) from the Japan Society for the Promotion of Science (JSPS) and Topcon. Author contributions: conception and design (N.U.A., S.O.); analysis and interpretation (N.U.A., S.O.); writing the article (N.U.A., S.O.); critical revision of the article (S.O., N.Y.); final approval of the article (N.U.A., S.O., A.A.E., A.Takahashi, A.O., H.T., K.Y., A.Tsujikawa, N.Y.); data collection (N.U.A., A.A.E., A.Takahashi); provision of materials (S.O., A.O., H.T., K.Y., A.Tsujikawa., N.Y.); statistical expertise (N.U.A., S.O.); obtaining funding (S.O.); literature search (N.U.A., S.O.).

REFERENCES

1. Mimoun G, Soubrane G, Coscas G. Macular drusen. J Fr Ophtalmol 1990;13(10):511–530.
2. Arnold JJ, Sarks SH, Killingsworth MC, Sarks JP. Reticular pseudodrusen. A risk factor in age-related maculopathy. Retina 1995;15(3):183–191.
3. Cohen SY, Dubois L, Tadayoni R, Delahaye-Mazza C, Debibie C, Quentel G. Prevalence of reticular pseudodrusen in age-related macular degeneration with newly diagnosed choroidal neovascularisation. Br J Ophthalmol 2007;91(3):354–359.
4. Sarks J, Arnold J, Ho IV, Sarks S, Killingsworth M. Evolution of reticular pseudodrusen. Br J Ophthalmol 2011;95(7):979–985.
5. Pumariega NM, Smith RT, Sohrab MA, Letien V, Souied EH. A prospective study of reticular macular disease. Ophthalmology 2011;118(8):1619–1625.
6. Schmitz-Valckenberg S, Alten F, Steinberg JS, et al. Reticular drusen associated with geographic atrophy in age-related

macular degeneration. Invest Ophthalmol Vis Sci 2011;52(9):5009–5015.
7. Klein R, Meuer SM, Knudtson MD, Iyengar SK, Klein BE. The epidemiology of retinal reticular drusen. Am J Ophthalmol 2008;145(2):317–326.
8. Ueda-Arakawa N, Ooto S, Nakata I, et al. Prevalence and genomic association of reticular pseudodrusen in age-related macular degeneration. Am J Ophthalmol 2013;155(2):260–269.e2.
9. Zweifel SA, Imamura Y, Spaide TC, Fujiwara T, Spaide RF. Prevalence and significance of subretinal drusenoid deposits (reticular pseudodrusen) in age-related macular degeneration. Ophthalmology 2010;117(9):1775–1781.
10. Lee MY, Yoon J, Ham DI. Clinical characteristics of reticular pseudodrusen in Korean patients. Am J Ophthalmol 2012;153(3):530–535.
11. Lee MY, Yoon J, Ham DI. Clinical features of reticular pseudodrusen according to the fundus distribution. Br J Ophthalmol 2012;96(9):1222–1226.
12. Querques G, Massamba N, Srour M, Boulanger E, Georges A, Souied EH. Impact of reticular pseudodrusen on macular function. Retina 2014;34(2):321–329.
13. Ooto S, Ellabban AA, Ueda-Arakawa N, et al. Reduction of retinal sensitivity in eyes with reticular pseudodrusen. Am J Ophthalmol 2013;156(6):1184–1191.e2.
14. Smith RT, Sohrab MA, Busuoic M, Barile G. Reticular macular disease. Am J Ophthalmol 2009;148(5):733–743.e2.
15. Spaide RF, Curcio CA. Drusen characterization with multimodal imaging. Retina 2010;30(9):1441–1454.
16. Ueda-Arakawa N, Ooto S, Tsujikawa A, Yamashiro K, Oishi A, Yoshimura N. Sensitivity and specificity of detecting reticular pseudodrusen in multimodal imaging in Japanese patients. Retina 2013;33(3):490–497.
17. Querques G, Querques L, Forte R, Massamba N, Coscas F, Souied EH. Choroidal changes associated with reticular pseudodrusen. Invest Ophthalmol Vis Sci 2012;53(3):1258–1263.
18. Sohrab MA, Smith RT, Salehi-Had H, Sadda SR, Fawzi AA. Image registration and multimodal imaging of reticular pseudodrusen. Invest Ophthalmol Vis Sci 2011;52(8):5743–5748.
19. Spaide RF, Koizumi H, Pozonni MC. Enhanced depth imaging spectral-domain optical coherence tomography. Am J Ophthalmol 2008;146(4):496–500.
20. Margolis R, Spaide RF. A pilot study of enhanced depth imaging optical coherence tomography of the choroid in normal eyes. Am J Ophthalmol 2009;147(5):811–815.
21. Imamura Y, Fujiwara T, Margolis R, Spaide RF. Enhanced depth imaging optical coherence tomography of the choroid in central serous chorioretinopathy. Retina 2009;29(10):1469–1473.
22. Fujiwara T, Imamura Y, Margolis R, et al. Enhanced depth imaging optical coherence tomography of the choroid in highly myopic eyes. Am J Ophthalmol 2009;148(3):445–450.
23. Manjunath V, Goren J, Fujimoto JG, Duker JS. Analysis of choroidal thickness in age-related macular degeneration using spectral-domain optical coherence tomography. Am J Ophthalmol 2011;152(4):663–668.
24. Chung SE, Kang SW, Lee JH, Kim YT. Choroidal thickness in polypoidal choroidal vasculopathy and exudative age-related macular degeneration. Ophthalmology 2011;118(5):840–845.
25. Jirarattanasopa P, Ooto S, Nakata I. Choroidal thickness, vascular hyperpermeability, and complement factor H in age-related macular degeneration and polypoidal choroidal vasculopathy. Invest Ophthalmol Vis Sci 2012;53(7):3663–3672.
26. Switzer DJ Jr, Mendonça LS, Saito M, et al. Segregation of ophthalmoscopic characteristics according to choroidal thickness in patients with early age-related macular degeneration. Retina 2012;32(7):1265–1271.
27. de Bruin DM, Burnes DL, Loewenstein J, et al. In vivo three-dimensional imaging of neovascular age-related macular degeneration using optical frequency domain imaging at 1050 nm. Invest Ophthalmol Vis Sci 2008;49(10):4545–4552.
28. Hirata M, Tsujikawa A, Matsumoto A, et al. Macular choroidal thickness and volume in normal subjects measured by swept-source optical coherence tomography. Invest Ophthalmol Vis Sci 2011;52(8):4971–4978.
29. Keane P, Ruiz-Garcia H, Sadda S. Clinical applications of long-wavelength (1,000-nm) optical coherence tomography. Ophthalmic Surg Lasers Imaging 2011;42(suppl):S67–S74.
30. Jirarattanasopa P, Ooto S, Tsujikawa A, et al. Assessment of macular choroidal thickness by optical coherence tomography and angiographic changes in central serous chorioretinopathy. Ophthalmology 2012;119(8):1666–1678.
31. Spaide RF. Age-related choroidal atrophy. Am J Ophthalmol 2009;147(5):801–810.
32. Ellabban AA, Tsujikawa A, Matsumoto A, et al. Three-dimensional tomographic features of dome-shaped macula by swept-source optical coherence tomography. Am J Ophthalmol 2013;155(2):320–328.e2.
33. Ellabban AA, Tsujikawa A, Matsumoto A, et al. Macular choroidal thickness and volume in eyes with angioid streaks measured by swept source optical coherence tomography. Am J Ophthalmol 2012;153(6):1133–1143.
34. Ellabban AA, Tsujikawa A, Matsumoto A, et al. Macular choroidal thickness measured by swept source optical coherence tomography in eyes with inferior posterior staphyloma. Invest Ophthalmol Vis Sci 2012;53(12):7735–7745.
35. Ellabban AA, Tsujikawa A, Ooto S, et al. Focal choroidal excavation in eyes with central serous chorioretinopathy. Am J Ophthalmol 2013;156(4):673–683.e1.
36. Ikuno Y, Kawaguchi K, Nouchi T, Yasuno Y. Choroidal thickness in healthy Japanese subjects. Invest Ophthalmol Vis Sci 2010;51(4):2173–2176.
37. Zweifel SA, Spaide RF, Curcio CA, Malek G, Imaura Y. Reticular pseudodrusen are subretinal drusenoid deposits. Ophthalmology 2010;117(2):303–312.e1.
38. Curcio CA, Messinger JD, Sloan KR, McGwin G, Medeiros NE, Spaide RF. Subretinal drusenoid deposits in non-neovascular age-related macular degeneration: morphology, prevalence, topography, and biogenesis model. Retina 2013;33(2):265–276.
39. Schmitz-Valckenberg S, Steinberg JS, Fleckenstein M, Visvalingam S, Brinkmann CK, Holz FG. Combined confocal scanning laser ophthalmoscopy and spectral-domain optical coherence tomography imaging of reticular drusen associated with age-related macular degeneration. Ophthalmology 2010;117(6):1169–1176.
40. Querques G, Canouï-Poitrine F, Coscas F, et al. Analysis of progression of reticular pseudodrusen by spectral domain–optical coherence tomography. Invest Ophthalmol Vis Sci 2012;53(3):1264–1270.
41. Spaide RF. Outer retinal atrophy after regression of subretinal drusenoid deposits as newly recognized form of late age-related macular degeneration. Retina 2013;33(9):1800–1808.

Biosketch

Naoko Ueda-Arakawa, MD, graduated from Kyoto University, Faculty of Medicine. She completed her residency program at Kyoto University Hospital and a fellowship at Osaka Red Cross Hospital, Osaka, Japan. She is now in a PhD program in the Department of Ophthalmology and Visual Sciences at Kyoto University under the supervisor of Professor Nagahisa Yoshimura. Her main interest is imaging analysis of macular diseases.

SUPPLEMENTARY TABLE 1. Comparison of Mean Age and Axial Length of Eyes With Reticular Pseudodrusen Among 3 Subgroups

	Group 1[a] (n = 20)	Group 2[a] (n = 10)	Group 3[a] (n = 8)	P[b]	P[c]	P[d]	P[e]
Mean age	77.6 ± 6.0	81.8 ± 7.9	81.1 ± 5.9	.183	.218	.389	.973
Mean axial length (mm)	23.2 ± 0.9	23.6 ± 0.7	23.8 ± 1.2	.268	.503	.296	.910

All values are presented as mean ± standard deviation.

[a]Group 1: eyes with reticular pseudodrusen and without late age-related macular degeneration (AMD); Group 2: eyes with reticular pseudodrusen and exudative AMD; Group 3: eyes with reticular pseudodrusen and geographic atrophy.

[b]Comparison between the 3 subgroups by 1-way analysis of variance.

[c]Comparison between Group 1 and Group 2 by the Tukey-Kramer test.

[d]Comparison between Group 1 and Group 3 by the Tukey-Kramer test.

[e]Comparison between Group 2 and Group 3 by the Tukey-Kramer test.

SUPPLEMENTARY TABLE 2. Comparison of Mean Choroidal Thickness and Volume of Eyes With Reticular Pseudodrusen Among 3 Subgroups

	Mean Choroidal Thickness (μm)			Mean Choroidal Volume (mm^3)						
Area[a]	Group 1[b] (n = 20)	Group 2[b] (n = 10)	Group 3[b] (n = 8)	Group 1[b] (n = 20)	Group 2[b] (n = 10)	Group 3[b] (n = 8)	P[c]	P[d]	P[e]	P[f]
Center	138.1 ± 52.2	148.0 ± 53.1	151.2 ± 45.9	0.11 ± 0.04	0.12 ± 0.04	0.12 ± 0.04	.787	.871	.811	.990
Inner temporal	145.9 ± 49.7	149.6 ± 47.1	162.6 ± 44.0	0.23 ± 0.08	0.23 ± 0.07	0.26 ± 0.07	.708	.979	.681	.832
Inner superior	138.8 ± 54.3	145.5 ± 46.4	155.0 ± 36.1	0.22 ± 0.09	0.23 ± 0.07	0.24 ± 0.06	.731	.934	.708	.910
Inner nasal	121.2 ± 49.2	130.9 ± 53.4	139.0 ± 34.5	0.19 ± 0.08	0.21 ± 0.08	0.22 ± 0.05	.654	.857	.646	.932
Inner inferior	129.2 ± 49.0	141.0 ± 61.7	147.7 ± 45.3	0.20 ± 0.08	0.22 ± 0.10	0.23 ± 0.07	.662	.827	.671	.959
Outer temporal	140.7 ± 39.2	144.9 ± 43.9	159.2 ± 38.4	0.75 ± 0.21	0.77 ± 0.23	0.84 ± 0.20	.552	.960	.516	.733
Outer superior	139.2 ± 44.8	139.6 ± 46.6	153.4 ± 35.9	0.74 ± 0.24	0.74 ± 0.25	0.81 ± 0.19	.721	1.000	.713	.781
Outer nasal	101.0 ± 36.6	107.5 ± 42.4	117.7 ± 22.9	0.53 ± 0.19	0.57 ± 0.22	0.62 ± 0.12	.539	.883	.507	.820
Outer inferior	130.4 ± 38.6	141.8 ± 62.4	143.6 ± 28.1	0.69 ± 0.20	0.75 ± 0.33	0.76 ± 0.15	.700	.781	.753	.996
Whole macula	129.3 ± 40.6	135.8 ± 46.3	145.4 ± 30.8	3.66 ± 1.15	3.84 ± 1.31	4.11 ± 0.87	.635	.910	.607	.868

All values are presented as mean ± standard deviation.

[a]Center = within 0.5 mm from the foveal center; Inner = 0.5–1.5 mm from the foveal center; Outer = 1.5–3.0 mm from the foveal center; Whole = within 3.0 mm from the foveal center.

[b]Group 1: eyes with reticular pseudodrusen and without late age-related macular degeneration (AMD); Group 2: eyes with reticular pseudodrusen and exudative AMD; Group 3: eyes with reticular pseudodrusen and geographic atrophy.

[c]Comparison between the 3 subgroups by 1-way analysis of variance.

[d]Comparison between Group 1 and Group 2 by the Tukey-Kramer test.

[e]Comparison between Group 1 and Group 3 by the Tukey-Kramer test.

[f]Comparison between Group 2 and Group 3 by the Tukey-Kramer test.

SUPPLEMENTARY TABLE 3. Comparison of Mean Choroidal Thickness in Each ETDRS Sector, 20 Eyes With Reticular Pseudodrusen Without Late Age-Related Macular Degeneration (Group 1) Were Grouped Into 2 Subgroups According to Whether Reticular Pseudodrusen Covered More or Less Than Half of Each Area

	Reticular Pseudodrusen Covered More Than Half of the Area		Reticular Pseudodrusen Covered Less Than Half of the Area		
Area[a]	Mean Choroidal Thickness (μm)	Number of Eyes	Mean Choroidal Thickness (μm)	Number of Eyes	P[b]
Center	125.1 ± 26.5	8	146.7 ± 63.8	12	.700
Inner temporal	141.1 ± 31.6	16	165.5 ± 100.2	4	.925
Inner superior	140.7 ± 57.0	18	122.0 ± 8.8	2	.529
Inner nasal	131.6 ± 55.9	13	101.9 ± 27.5	7	.322
Inner inferior	129.5 ± 34.2	13	128.7 ± 72.5	7	.191
Outer temporal	141.6 ± 20.5	13	138.9 ± 63.4	7	.122
Outer superior	141.6 ± 44.7	19	93.6	1	N/A
Outer nasal	103.0 ± 41.5	12	97.9 ± 30.2	8	.758
Outer inferior	130.4 ± 28.2	9	130.4 ± 46.9	11	.621

All values are presented as mean ± standard deviation.

[a]Center = within 0.5 mm from the foveal center; Inner = 0.5–1.5 mm from the foveal center; Outer = 1.5–3.0 mm from the foveal center; Whole = within 3.0 mm from the foveal center.

[b]Mann–Whitney U test.

Jpn J Ophthalmol (2014) 58:155–165
DOI 10.1007/s10384-013-0295-z

THE OFFICIAL INTERNATIONAL JOURNAL OF THE JAPANESE OPHTHALMOLOGICAL SOCIETY

CLINICAL INVESTIGATION

Multimodal evaluation of macular function in age-related macular degeneration

Ken Ogino · Akitaka Tsujikawa · Kenji Yamashiro · Sotaro Ooto · Akio Oishi · Isao Nakata · Masahiro Miyake · Ayako Takahashi · Abdallah A. Ellabban · Nagahisa Yoshimura

Received: 20 June 2013 / Accepted: 29 October 2013 / Published online: 12 December 2013

Abstract
Objective To evaluate macular function using multimodality in eyes with age-related macular degeneration (AMD) at various stages.
Methods Macular function in 20 control eyes (20 subjects), 17 eyes (17 patients) with large drusen, 18 eyes (18 patients) with drusenoid pigment epithelial detachment (PED), and 19 eyes (19 patients) with neovascular AMD was examined using a Landolt chart for visual acuity; retinal sensitivity was measured by microperimetry; and focal macular electroretinography (fmERG) was performed. In all of these eyes, retinal morphology was examined using optical coherence tomography.
Results Eyes with neovascular AMD showed morphologic changes in the neurosensory retina as well as marked deterioration of macular function in all parameters measured with a Landolt chart, fmERG, and microperimetry. Eyes with large drusen showed only minimal morphologic changes in the neurosensory retina. In this large drusen group, although retinal sensitivity at the central point was significantly decreased ($P = 0.0063$), the other parameters of macular function were well preserved. In eyes with drusenoid PED, the structure of the neurosensory retina was well preserved, while the foveal thickness was significantly increased ($P = 0.013$). The macular function of these eyes was significantly deteriorated, with the VA, amplitude of the a-wave and b-wave, and retinal sensitivity being markedly decreased. In addition, the area of PED correlated with the latency of the a-wave and b-wave and with the retinal sensitivity within the central 4° or 8° region.
Conclusion Multimodal evaluation demonstrated a significant decrease in macular function in drusenoid PED and in neovascular AMD.

Keywords Age-related macular degeneration · Drusenoid pigment epithelial detachment · Drusen · Focal macular electroretinography · Microperimetry

K. Ogino · A. Tsujikawa (✉) · K. Yamashiro · S. Ooto · A. Oishi · I. Nakata · M. Miyake · A. Takahashi · A. A. Ellabban · N. Yoshimura
Department of Ophthalmology and Visual Sciences, Kyoto University Graduate School of Medicine, Sakyo-ku, Kyoto 606-8507, Japan
e-mail: tujikawa@kuhp.kyoto-u.ac.jp

Introduction

Age-related macular degeneration (AMD) is one of the leading causes of visual impairment and an intensive therapeutic target in developed countries [1–6]. Drusen or drusenoid pigment epithelium detachment (PED), which is a prodrome lesion of advanced AMD, does not usually cause severe loss of visual acuity (VA), but it is the subsequent development of choroid neovascularization (CNV) that so often causes the central visual disturbance. So far, however, visual impairment due to AMD has been evaluated primarily by VA measurement alone. Indeed, VA measurement is essential to evaluate visual function, but it reflects only foveal function. Lesions of AMD, including drusen, CNV, serous retinal detachment, subretinal hemorrhage, and PED, are seen not only beneath the fovea, but also in the larger macular area, which leads to the macular dysfunction [7].

To evaluate visual function of the entire macular area, simultaneous use of focal macular electroretinography (fmERG) and of microperimetry have recently been reported [8, 9]. fmERG enables measurement of macular

function throughout its entirety, even in patients with poor fixation, by monitoring through an infrared camera and manual adjustment of the stimulus to the macular area [10]. Microperimetry allows functional evaluation of selected points throughout the macular area [11, 12]. During this test, the autotracking function corrects for shifts in the measurement position caused by small, involuntary movements. Recent studies using microperimetry have shown that early or advanced AMD often accompanies the severe reduction in sensitivity of the macular area [13–21]. With the use of microperimetry, Yodoi et al. [22] reported a functional reduction in the macular area of eyes with subfoveal polypoidal choroidal vasculopathy, which is a variant of neovascular AMD. In their report, macular function improved after photodynamic therapy with concomitant recovery of the subjective symptoms, despite there being no improvement in VA.

Other recent studies with microperimetry or ERG have evaluated macular function in eyes with AMD and have reported that it is impaired—even in eyes with drusen alone [23, 24]. Indeed, each modality has both advantages and limitations. To evaluate visual function effectively, it would be of help to measure retinal function within the macular area using the multimodality approach. So far, however, little information is available on the multimodal evaluation of visual function in eyes with AMD. Therefore, this study was designed to evaluate the macular function using multimodality in eyes with AMD at various stages, including those with large drusen, drusenoid PED, and neovascular AMD.

Patients and methods

In this prospective study, we performed multimodal evaluation of macular function in eyes with AMD at various stages; the eyes comprised 17 (17 patients) with large drusen, 18 (18 patients) with drusenoid PED, and 19 (19 patients) with neovascular AMD (8 eyes with typical AMD and 11 eyes with polypoidal choroidal vasculopathy). Eyes with large drusen were judged by the presence of multiple large drusen (>125 μm) within 3,000 μm of the center of the macula on fundus photographs. The diagnostic criteria of drusenoid PED were confluent drusen, with a focal area of PED involving the macular area, with a minimum size of 1/2 disc diameter [25], and without CNV detected on ophthalmoscopy or fluorescein and indocyanine green angiography. Neovascular AMD was diagnosed on the basis of fluorescein and indocyanine green angiography, which showed an exudative change with CNV. In the current study, eyes with central geographic atrophy were excluded. We also recruited 20 eyes (20 subjects) as an age-adjusted control group. The criteria for the eyes, including for the control eyes, were as follows: ≥1.0 VA on a Landolt chart, <10 small drusen (<63 μm) within 3,000 μm of the center of the macula on the fundus photograph, normal morphology of the fovea as seen with optical coherence tomography (OCT), and absence of central geographic atrophy or CNV.

This study was approved by the institutional review board of Kyoto University Graduate School of Medicine and adhered to the tenets of the Declaration of Helsinki. Written informed consent for research participation was obtained from each subject before examination.

Each subject underwent a comprehensive ophthalmologic examination, including measurement of best-corrected VA on a Landolt chart, determination of intraocular pressure, indirect ophthalmoscopy, and slit-lamp biomicroscopy with a contact lens. In each subject, 45° digital fundus photographs were obtained using a digital fundus camera (TRC-50LX; Topcon, Tokyo, Japan; 3,216 × 2,136 pixels) after pupil dilatation, and the macular area was examined with a Spectralis HRA + OCT device (Heidelberg Engineering, Heidelberg, Germany). Each patient with large drusen, drusenoid PED, or neovascular AMD underwent fluorescein and indocyanine green angiography with a confocal laser scanning system (HRA-2; Heidelberg Engineering). In each eye, macular function was examined by fundus-monitored microperimetry and fmERG recording.

Retinal sensitivity within the macular area was examined with a fundus-monitored microperimeter [Micro Perimeter 1 (MP1); Nidek, Gamagori, Japan]. A 4-2-staircase strategy with Goldmann III-sized stimuli was used, and 57 stimulus locations within a 10° radius were examined by microperimetry. Each stimulus was located according to the measurement points on the Humphrey 10-2, with some additional points. The white background illumination was set at 1.27 cd/m^2. The differential luminance, defined as the difference among the stimulus luminance, and background luminance, was 127 cd/m^2 at 0-dB stimulation, and the maximum stimulus attenuation was 20 dB. The stimulus duration was 200 ms (ms), and the fixation target varied in size according to the VA of the patient. There were 17 and 37 measurement points within the central circles with radii of 4° and 8°, respectively.

The fmERG recording procedure has been previously described in detail [8, 9]. Briefly, after maximal dilatation of the pupils of both eyes, a Burian–Allen bipolar contact lens electrode (Hansen Ophthalmic Laboratories, Iowa City, IA, USA) was placed in the conjunctival sac of each eye under topical anesthesia. A chloride silver electrode was attached to the left earlobe to serve as the ground electrode. The fmERG was elicited by circular stimuli positioned on the macular area, using a prototype of the ER-80 (Kowa, Tokyo, Japan), which consisted of an

Table 1 Background, foveal thickness, and macular function of control eyes, eyes with large drusen, eyes with drusenoid pigment epithelial detachment, and eyes with neovascular age-related macular degeneration

	Controls	Large drusen	Drusenoid PED	Neovascular AMD	*P* value
Sex (male/female)	16/4	11/6	18/0	16/3	0.054
Phakia/pseudophakia	14/6	9/8	13/5	12/7	0.627
Age, years	82.0 ± 3.2	80.7 ± 5.2	78.9 ± 5.0	77.3 ± 6.9	0.040
Visual acuity, logMAR	−0.07 ± 0.07	0.05 ± 0.14	0.16 ± 0.18	0.42 ± 0.42	<0.0001
Foveal thickness, μm					
ILM to RPE	224 ± 27	196 ± 40	200 ± 49	384 ± 256	<0.0001
ILM to Bruch membrane	224 ± 27	231 ± 36	377 ± 164	533 ± 263	<0.0001
Amplitude of fmERG, μV					
a-wave	1.73 ± 0.65	1.35 ± 0.49	1.21 ± 0.67	0.87 ± 0.58	0.0005
b-wave	3.14 ± 0.89	2.55 ± 0.91	2.20 ± 1.09	1.37 ± 1.04	<0.0001
Latency of fmERG, ms					
a-wave	23.18 ± 1.28	23.67 ± 1.58	24.39 ± 1.77	25.76 ± 3.39	0.040
b-wave	42.05 ± 2.27	45.44 ± 3.87	45.22 ± 3.71	48.87 ± 7.38	0.0005
Retinal sensitivity, dB					
Center point	14.78 ± 3.52	9.94 ± 3.86	3.82 ± 3.43	5.37 ± 6.31	<0.0001
Within 4°	16.50 ± 2.01	13.35 ± 3.57	6.83 ± 4.39	5.78 ± 6.27	<0.0001
Within 8°	16.13 ± 2.10	13.66 ± 3.32	9.19 ± 3.94	6.76 ± 6.23	<0.0001

PED pigment epithelium detachment, *AMD* age-related macular degeneration, *fmERG* focal macular electroretinography, *ILM* internal limiting membrane, *RPE* retinal pigment epithelium

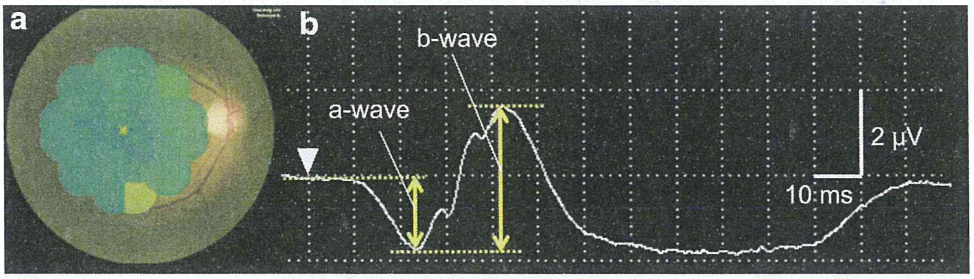

Fig. 1 Macular function in a healthy control eye. Retinal sensitivity map obtained by microperimetry (**a**) and focal macular electroretinography (**b**). *White arrowhead* beginning of stimulus; *yellow arrow* amplitude of each wave of focal macular electroretinogram

infrared camera (Kowa) and a stimulation system (Mayo Corp., Nagoya, Japan). The luminance values of the white stimulus light and the background illumination were 181.5 and 6.9 cd/m^2, respectively. The stimulus within the 7.5°-radius circle was centered on the fovea, as observed through the infrared camera. The fmERG was recorded using 5-Hz rectangular stimuli (100 ms with the light on and 100 ms with the light off). The recording (200 responses) was carried out in triplicate to confirm the reproducibility of the results; thus, a total of 600 responses were averaged by the signal processor (Neuropack MEB-2204; Nihon Kohden, Tokyo, Japan). The fmERG response was digitized at 10 kHz with a band-pass filter of 5–500 Hz for the a-wave and the b-wave. The amplitudes of the a- and b-waves were measured from baseline to the peak of the a-wave and from the trough of the a-wave to the peak of the b-wave, respectively. Latency was defined as the time from the beginning of stimulation to the peak of each component.

For the OCT images, the foveal thickness in each eye was determined in the following two ways: the distance between the internal limiting membrane (ILM) and the outer border of the RPE or the distance between the ILM and the Bruch membrane. In eyes with drusenoid PED, we also measured the height and area of the PED. For the sequential OCT images, the height of the PED was defined as the maximal distance between the outer border of the RPE and the Bruch membrane (sometimes outside the fovea). For the late-phase indocyanine green angiogram, the area of the PED was measured using software built into the HRA-2. Briefly, drusenoid PED was observed as a dark area on the late-phase indocyanine green angiogram, and

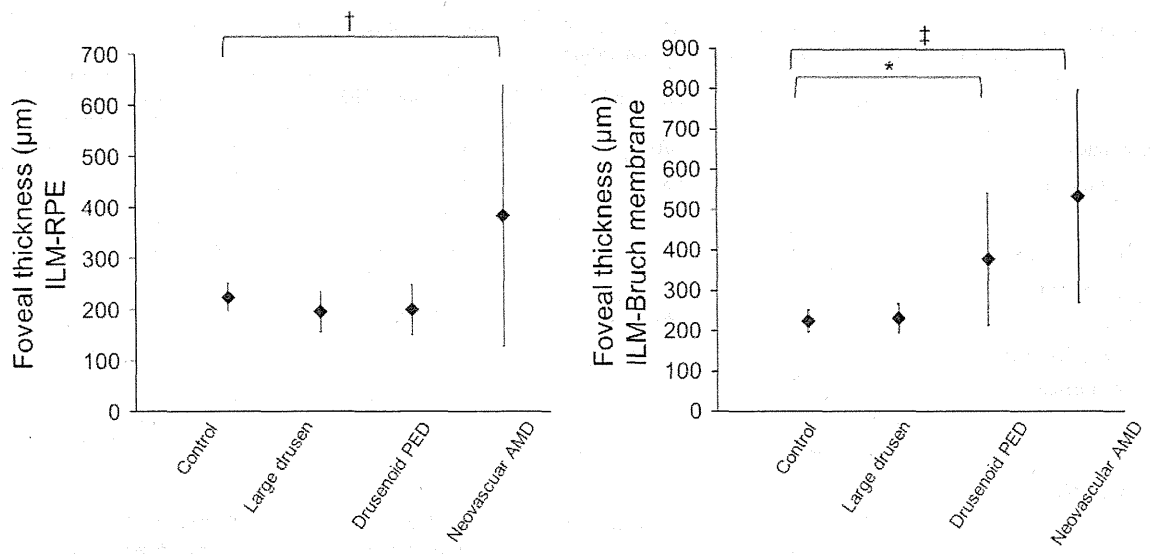

Fig. 2 Foveal thickness of control eyes, eyes with large drusen, eyes with drusenoid pigment epithelial detachment, and eyes with neovascular age-related macular degeneration. $^{*}P < 0.05$, $^{\dagger}P < 0.01$, $^{\ddagger}P < 0.0001$, as compared with control eyes. *P* values were calculated by the Dunnet test. *ILM* internal limiting membrane, *RPE* retinal pigment epithelium, *PED* pigment epithelium detachment, *AMD* age-related macular degeneration

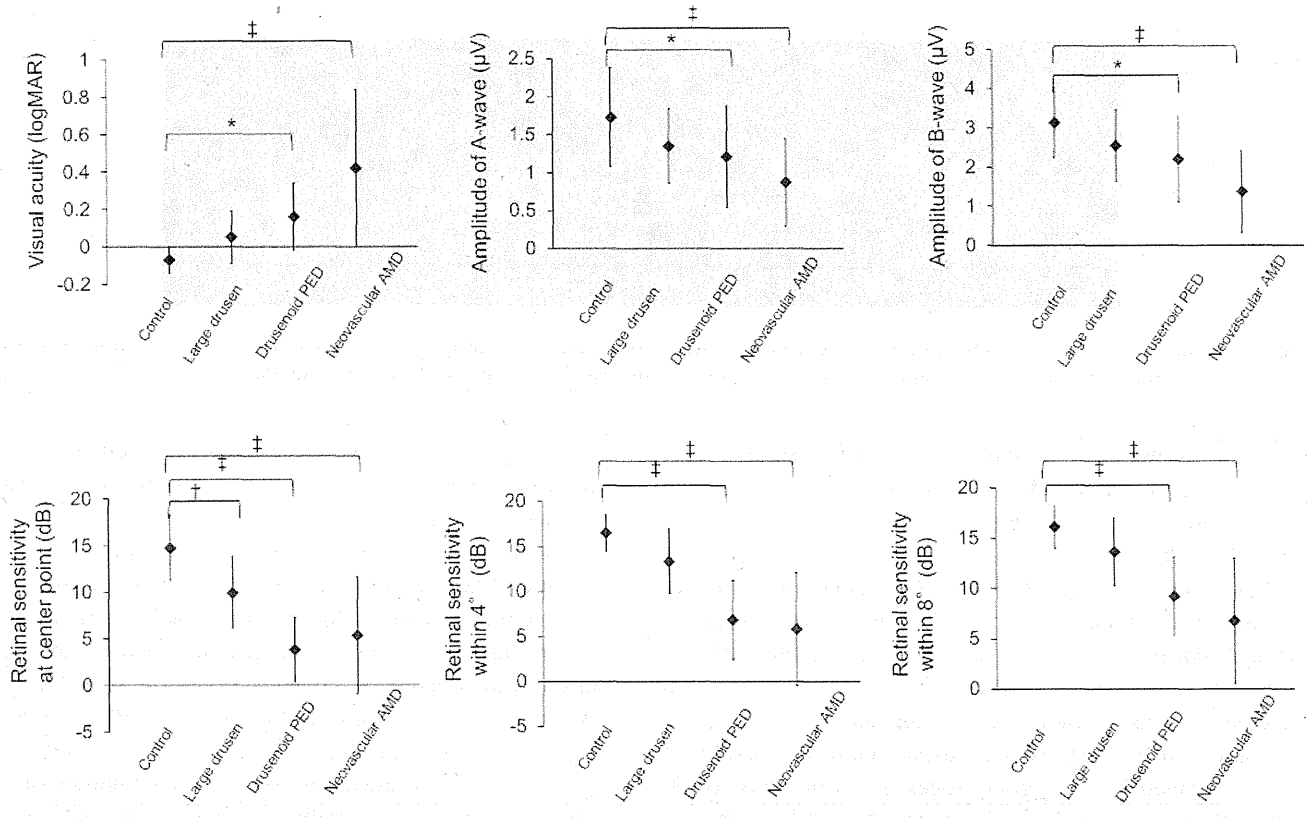

Fig. 3 Macular function measured with multimodality in control eyes, eyes with large drusen, eyes with drusenoid pigment epithelial detachment, and eyes with neovascular age-related macular degeneration. $^{*}P < 0.05$, $^{\dagger}P < 0.01$, $^{\ddagger}P < 0.0001$, as compared with control eyes. *P* values were calculated by the Dunnet test. *LogMAR* logarithm of the minimum angle of resolution, *PED* pigment epithelium detachment, *AMD* age-related macular degeneration

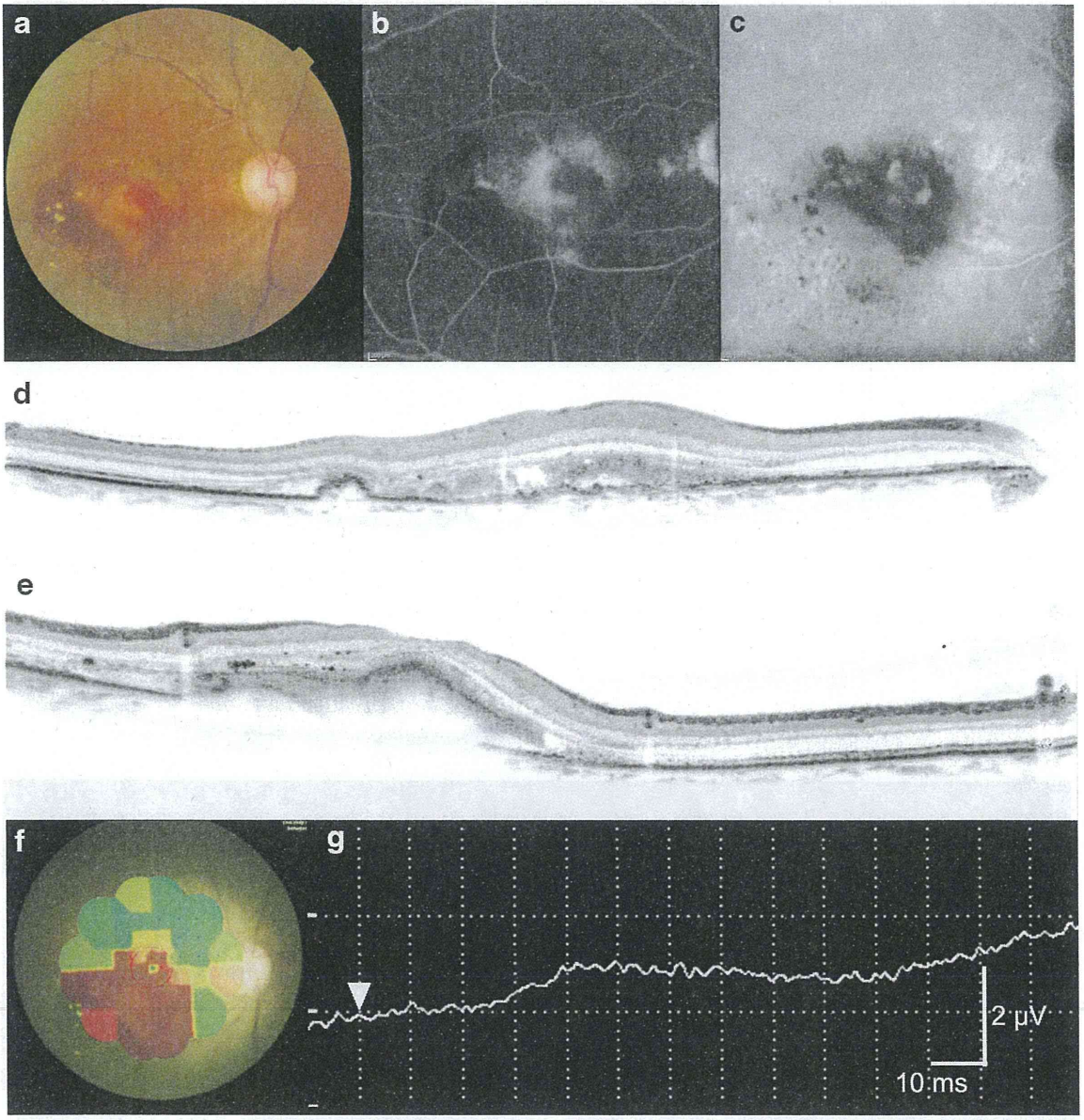

Fig. 4 Macular function in an eye with neovascular age-related macular degeneration. **a** Fundus photograph shows submacular hemorrhage (0.15 on a Landolt chart, OD). **b**, **c** *Fluorescein* and *indocyanine green* angiograms reveal subfoveal choroidal neovascularization. *Horizontal* **d** and *vertical* **e** sections obtained with OCT show subretinal fluid. **f** Retinal sensitivity map obtained with microperimetry shows a substantial reduction of retinal sensitivity in the macular function. **g** Focal macular electroretinogram shows a substantial reduction in amplitude of all waves. *Arrowhead* beginning of stimulus

the edge of this central dark area was traced manually. The surrounding small dark lesions (drusen) isolated from the central PED were not included.

Statistical analysis was performed using PASW Statistics version 17.0 software (SPSS, Chicago, IL, USA). All values were expressed as means ± standard deviations. The best-corrected VA was measured using a Landolt chart and converted to the logarithm of the minimum angle of resolution (logMAR). To clarify differences from the healthy controls, all mean values between groups were compared using one-way analysis of variance and post hoc Dunnet tests. Bivariate analysis was done with the Pearson product moment correlation.

Results

Table 1 shows the characteristics of the study populations. Although the controls (82.0 ± 3.2 years) were significantly older than the patients with neovascular AMD (77.3 ± 6.9 years, $P = 0.019$), there was no significant difference in the gender or lens status of groups. In the